Risk Assessment and Forecasting of Indian Summer Monsoon for Agricultural Drought Impact Planning

Balaji Rajagopalan

June 2009

Completion Report No. 215

Colorado State University

This report was financed in part by the U.S. Department of the Interior, Geological Survey, through the Colorado Water Institute. The views and conclusions contained in this document are those of the authors and should not be interpreted as necessarily representing the official policies, either expressed or implied, of the U.S. Government.

Additional copies of this report can be obtained from the Colorado Water Institute, E102 Engineering Building, Colorado State University, Fort Collins, CO 80523-1033 970-491-6308 or email: cwi@colostate.edu, or downloaded as a PDF file from http://www.cwi.colostate.edu.

Risk Assessment and Forecasting of Indian Summer Monsoon for Agricultural Drought Impact Planning

Rajagopalan Balaji,
Associate Professor of Civil, Environmental and Architectural Engineering University of Colorado, Boulder

Preamble

"The wild monsoon winds blow with abandon, swaying everything in their path... rivers flow and flowers bloom in celebration of the monsoon, as the world is transformed under its spell," notes poet S. P. Kurada in the PBS documentary "Monsoon". The author's sentiments about the monsoon are no exaggeration, for the socio-economic destiny of millions of people in the Indian sub-continent are tightly bound to the timely arrival and an even spatial distribution of the Indian summer monsoon. Most parts of the sub-continent receive almost all their annual rainfall during the summer monsoon season (June – Sept.). However, the amount of rainfall and its spatial distribution over the sub-continent varies significantly from year to year (also known as inter-annual variability), and also within the season (intra-seasonal variability). The monsoon greatly impacts, agriculture (more than 50 percent of which is rain fed), power generation (more that 50 percent of which is hydroelectric from rain fed rivers), and consequently, prices of essential commodities. Thus, it affects the entire spectrum of life - social, political and financial. Hence, understanding the variability of the monsoon (both inter-annual and intra-seasonal), being able to predict its strength and spatial distribution and the associated hydrologic aspects is of crucial importance to the well being of one-billion of the world's population. This served as a strong motivation for the proposed research.

Objectives of the study

Planning for drought and food security is critical for India's economy and societal well being. This fact is greatly underscored by the increasing population, scarce natural resources and significant dependency on the vagaries of the summer monsoon. We proposed a study to aid this planning effort by developing tools for intra-seasonal, subnational drought risk forecasting. To this end, the objectives were two fold – 1) to quantify the probability, on average, of the occurrence of agriculturally significant dry spells and 2) to provide a tool for predicting the risk each year based on prevailing conditions of the global climate system.

Report Layout

The proposed methodology and the tasks are first described, followed by the results and discussion for future extensions. All the analyses were performed using the free software R and links to various codes and a number of figures not presented in report are listed in the appendix.

Methodology

Not much research has been performed on the intra-seasonal variability of the monsoon. Nonetheless, the subseasonal variability is crucial to agricultural and water resources applications. For example, farmers are particularly interested in the rainfall

spells in the first couple of weeks of June (the typical sowing period), and they do not like to see severe rains in August and September when the crop would be matured. While the focus of current practice has mainly been to predict seasonal rainfall totals, clearly, the subseasonal attributes are crucial for sectoral applications. There is a strong need for a systematic analysis of subseasonal variability. Our findings will make possible increased specificity of monsoon forecasts in space and time. Two broad tasks were carried out which are described below.

Task A - Diagnostics and Risk assessment

The Indian Meteorological Department recently completed a daily, gridded national rainfall data set at 0.5 degree resolution (about 50 km) for the period 1951-2007 (Rajeevan et al., 2006). These unprecedented data make possible for the first time a spatially continuous and explicit characterization of the frequency of drought and dry spell occurrence over India based on 57 years of observations. From these daily rainfall data, at each grid location, for each month of the monsoon season, the following set of frequency and probability attributes were derived (0.5 mm of rainfall was used as the threshold to define a 'wet day'):

(i) Number of wet and dry spells (a wet spell being a series of consecutive days with measurable rainfall above a specified threshold, and a dry spell being a consecutive series of days with rainfall below a minimum threshold)

(ii) Probability distributions of wet and dry spells of various lengths

(iii) Probability of transition between wet and dry spells. The probability of transiting from a wet day to a dry day or vice-versa was computed for the desired periods (e.g., June, July, first half of June, second half of June, etc.).

(iv) Probability of extreme events

(v) Rainfall deficit. This was computed as the difference between the total seasonal (June-Oct) rainfall and the amount of rainfall required for a particular crop. The average deficit with respect to a particular crop was computed and spatially mapped.

(vi) In addition to the above we also computed the monthly and seasonal rainfall and the Julian days of accumulation of various thresholds of precipitation in each year and consequently, investigated the temporal trends in these attributes. The goal was to identify any shifts in seasonality.

Thus, computed attributes were then spatially mapped to provide 'risk estimates'. Also, the spatial maps were developed for different conditions of the global climate system – e.g., El Nino years, La Nina years, etc.

Deliverables

(i) Spatial maps of probabilities (risks) of various agriculturally significant rainfall events from the historical data. These provide a good sense of the 'static' risk relevant for agriculture planning.

(ii) Similar spatial maps of these rainfall events conditioned on large scale climate features. For instance, if ENSO conditions are found to be a strong driver of these attributes, spatial maps of probabilities of these attributes for El Nino, La Nina and neutral years were developed. Planners may refer to whichever map corresponds to currently prevailing conditions of the equatorial Pacific.

Results – Risk Maps

Spell Risk

A sampling of the results is presented and discussed below and links to all the maps generated are provided. Spatial maps of the probability of a wet spell greater than seven days during the month of July (the month in which more than 40 percent of the annual rainfall is received in much of the country), for all the years and for the El Nino years, are shown in Figures 1a and 1b, respectively. Wet spells of a week or longer are necessary for robust crop growth – especially during the maturing period of July – hence, the choice of this metric. It can be seen that there is a reduction in the probability of a wet spell during El Nino years over the Eastern Indo-Gangetic plains and also along the Western Ghats. The probabilities are closer to zero over Northwestern India (i.e. the desert region) and the Southern Peninsula (which gets the monsoon rains during Oct-Dec). We also computed these probabilities for the first half and second half of each month to provide estimates on a bi-weekly basis for planning. All of these maps are available at http://civil.colorado.edu/~verdina/Risk%20Maps/

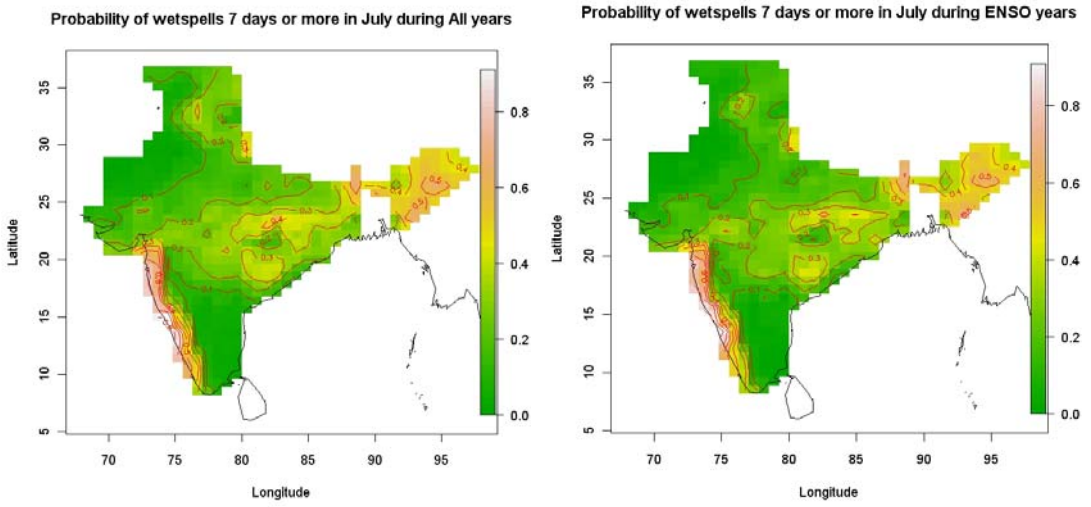

(a) (b)

Fig 1*: Spatial maps of probability of wet spells longer than or equal to seven days (a) during June and (b) during July for El Nino years.*

* more maps available: http://civil.colorado.edu/~verdina/Risk%20Maps/

Average wet days

The average number of wet and dry days was computed from the daily rainfall data at each location for bi-weekly periods in the season. These maps can be very useful in providing an estimate of the number of wet days that can be expected and thus help in crop management at various stages of growth. Figure 2 shows the average wet days for the second half of July for all the years and for El Nino years. We see that the during El Nino years there is a slight reduction in the average number of wet days in the central and Indo-Gangetic regions.

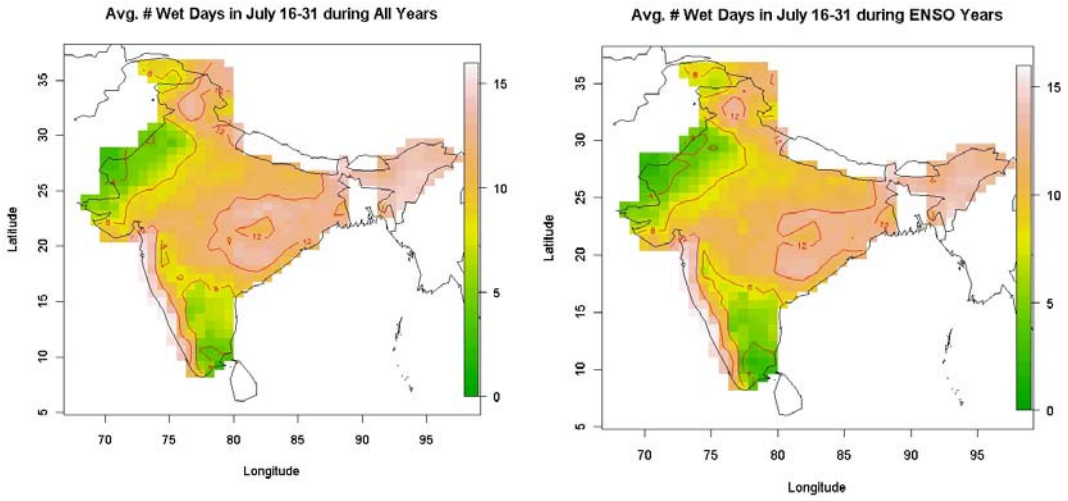

(a) (b)

Figure 2. *Average number of wet days during the second half of July (a) based on all the years and (b) based on El Nino years. Maps for other periods can be found at http://civil.colorado.edu/~verdina/Wet%20Days/*

Transition Probabilities

Transition probabilities provide crucial information on the probability of transiting from a wet day/spell to a dry day/spell, and vice-versa, and consequently provide the probabilities of various spell lengths. Transition probabilities were computed on bi-weekly period through the monsoon season. Transition probabilities for the first bi-week of July, based on the all the years and for El Nino years, are shown in Figure 3. It can be seen that there is a increased probability to transition from a wet day to a dry day during El Nino years (Fig 3b) over much of the country – especially central India, Indo-Gangetic plains, Western Ghats and Western India. Maps for all the periods can be found in the link provided in the figure caption.

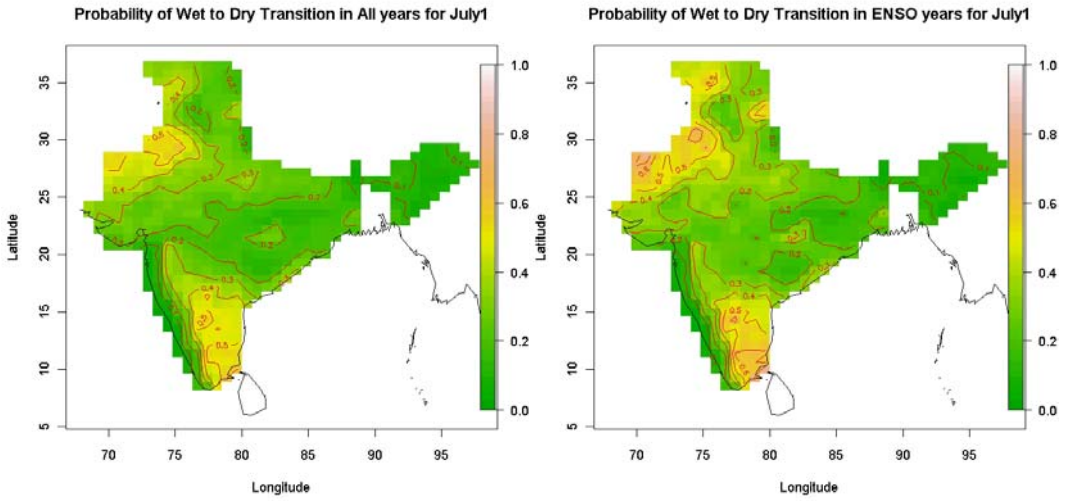

(a) (b)

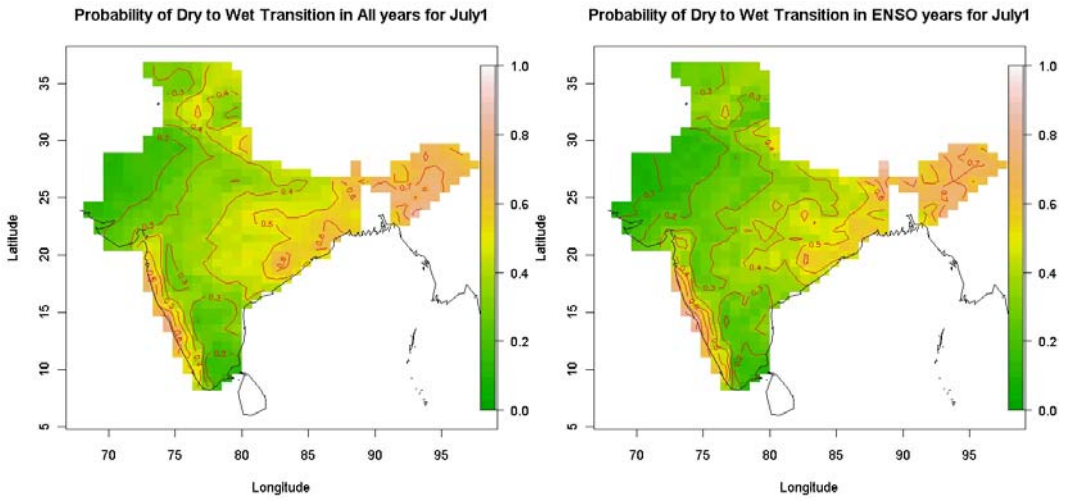

(c) (d)

Figure 3*. Spatial maps of transition probabilities for the first bi-week of July (a) transition from a wet to a dry day, (b) same as (a) but for El Nino years, (c) transition from dry to wet day and (d) same as (c) but for El Nino years.*

* maps for the rest of the monsoon season are available at http://civil.colorado.edu/~verdina/Transition%20Plots/

The transition probabilities (Wilks, 2006) can be used to generate sequences of wet and dry days based on seasonal forecast (e.g., ENSO) that can be used to obtain statistics of the precipitation attributes and also can be used to drive crop models to obtain insights into the yields in the upcoming season, immensely useful for resource planning.

Average seven day Annual maximum rainfall

At each grid point annual maximum seven day total rainfall was computed. The average of this over all the years is mapped spatially (Figure 4). Then aim of this attribute is to capture the heavy rainfall event which is important to replenish the soil moisture and also to aid in crop growth.

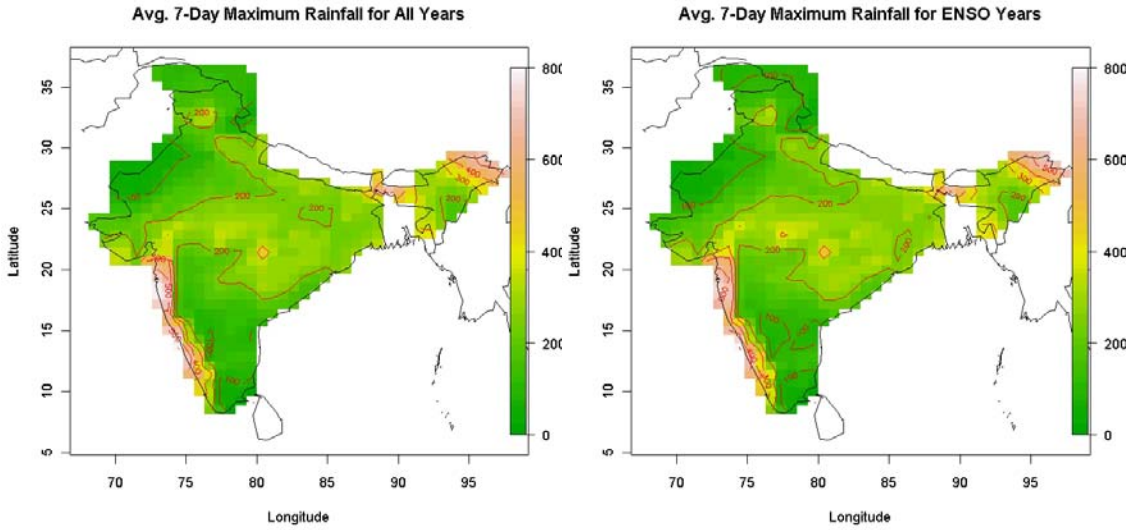

Figure 4. *Average seven day maximum rainfall (a) for all years and (b) during El Nino years, in millimeters.*

The annual maximum seven day rainfall is generally lower during El Nino years over much of Central and Northern India. This is consistent with the other risk maps described above.

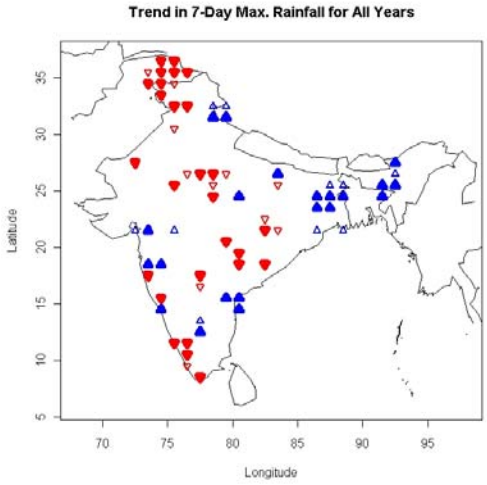

The historical trend in annual maximum seven day rainfall was also determined for all grids points. Figure 5 shows the results. Notice that there is a decreasing trend over much of the country indicating that in recent years there is a tendency for reduced wet events. This has substantial negative impact on crop growth.

We also developed spatial maps of rainfall of various return periods from fitting a Generalized Extreme Value (GEV) distribution (Katz et al., 2002). These show interesting features and can be of immense use in flood mitigation strategies – see e.g. the 100 year return period maps.

http://civil.colorado.edu/~verdina/7%20day%20maximum/100-year-event.jpg

Figure 5. *Trend in seven day annual maximum rainfall. Filled triangles are significant at 95 percent confidence and unfilled at 90 percent. The upward blue arrows indicate an increasing trend and downward red arrows indicate a decreasing trend.*

Average Deficit Rainfall

Since much of the agriculture in India is rain fed, crops not only need sufficient wet spells for a good yield, but also sufficient rainfall. Rainfall deficits over the entire growing season (June-Oct.) at each grid point with respect to a successful rice crop (which requires 1200 mm of rain) is computed for each, and the average deficit is spatially mapped for all the years and El Nino years in Figure 6. The rainfall deficits with respect to rice crops are lowest in Central India, Indo-Gangetic plains and North Eastern parts of the country. The deficits are larger in the Peninsular and Northwestern region. During El Nino years the average deficit is higher, consistent with a weaker monsoon.

The deficit maps can be computed for various crops of interest and also at various stages of crop growth. These in conjunction with wet spell risks can be very useful in identifying the "best locations" for various crops and thus, guide towards a sustainable agricultural policy.

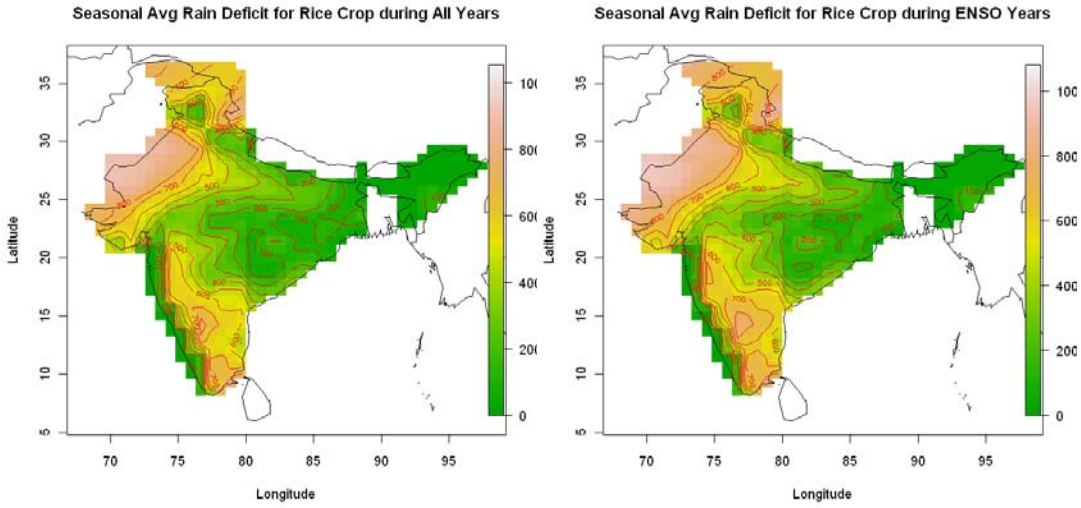

(a) (b)

Figure 6*. Average seasonal rainfall deficit for rice crop during the growing season (June-Oct.) for (a) all years and (b) El Nino years.*

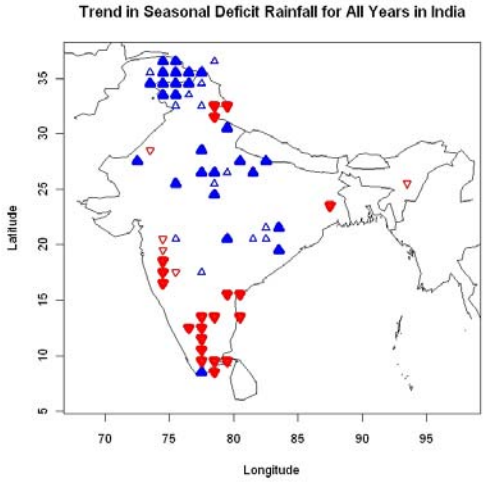

Temporal trend (1951-2007) of the seasonal rainfall deficit for rice crop is shown in Figure 7. We find that the deficit is increasing over much of central and North India while there is a decrease in the peninsular region – although the peninsular region does not get much rainfall during the summer monsoon.

Figure 7*. Same as Figure ,5 but for seasonal rainfall deficit for rice crop during the growing season (June-Oct).*

Seasonality Shifts

There have been recent reports that the seasonality of the monsoon is advancing (occurring earlier). In order to investigate the seasonality shifts, trends in monthly rainfall were computed for May (pre-monsoon month) and July (monsoon month) rainfall. Figure 8 clearly shows that there is a significant increasing trend in May rainfall over much of the country – especially the Central and Northern India and a corresponding decreasing trend in July. This is alarming in that July is the critical month as the country receives over 40 percent of the annual rainfall.

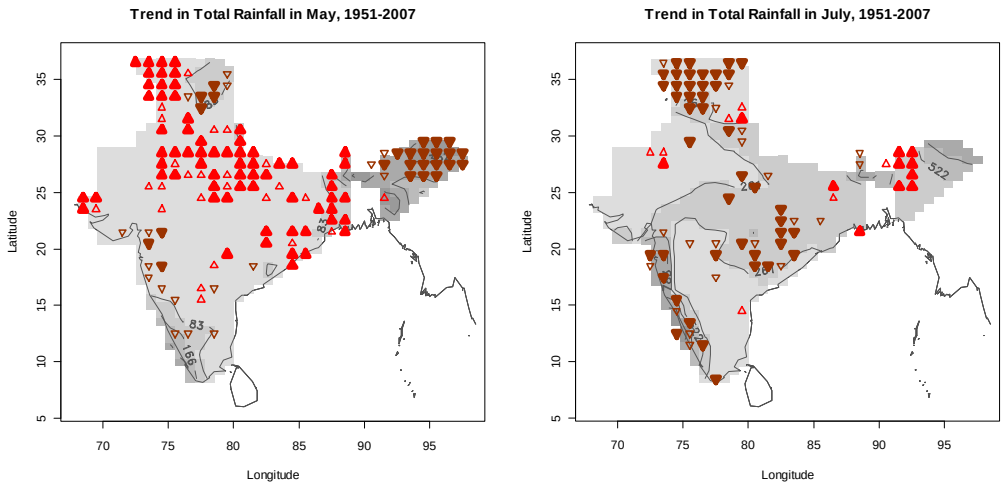

Figure 8. *Trend in May and July monthly rainfall totals over the period 1951-2007. The upward red arrows indicate an increasing trend and downward red arrows indicate a decreasing trend.*

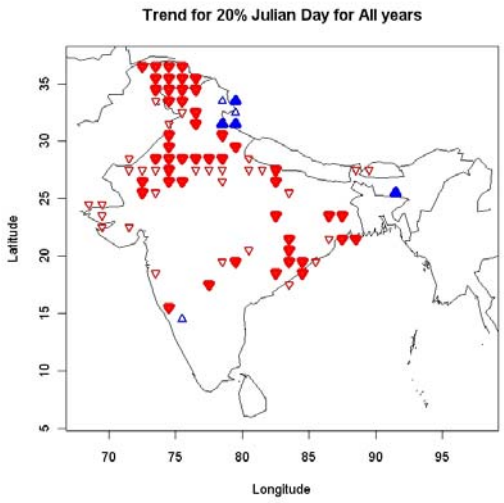

This is further corroborated by the trends in Julian day when 20 percent of the annual rainfall occurs (Figure 9). The significant decreasing trend indicates that the day is advancing – indicative of advancing rains and seasonality.

Figure 9. *Trend in the Julian day by when 20 percent of the annual rainfall is accumulated.*

The upward blue arrows indicate an increasing (later) trend and downward red arrows indicate a decreasing (earlier) trend.

These insights into the advancement of season are very useful for providing guidelines for sowing. If the seasonality is shifting early then an early planning might be considered.

Trends in Julian day of other accumulation thresholds also reveal similar behavior and can be found at http://civil.colorado.edu/~verdina/Trend%20in%20Julian/

The above collection of risk information from the daily precipitation will be extremely useful in short term disaster mitigation strategies (floods and droughts) and also for long term sustainable policy making. In particular, at seasonal time scales based on large scale climate forecast, the risk information can be used to generate an ensemble of daily weather sequences (e.g., Apipattanavis, et al., 2007) to provide regional risk estimates, and coupling these with crop models can provide yield projections useful for planning (Apipattanavis, 2008). These can also be estimated in the face of changing climate (Podesta et al., 2009; Katz et al., 2002).

Task B – Risk Prediction

Most of the focus of current practice has been on the seasonal prediction of all-India summer rainfall. While this is worthwhile, it is of limited usefulness for planning and managing of resources in several parts of India, as the spatial variability of rainfall distribution is quite high. Consequently, forecasting tools are needed for individual regions. To this end, predictive tools were developed for forecasting seasonal rainfall and the probability of agriculturally important intra-seasonal rainfall events for planning (as identified in Task A). The resulting ensemble forecasting tools can help provide risk outlooks each year.

Finding Predictors

The first step in forecasting is finding significant predictors from the large scale land-ocean-atmosphere system. We computed the regional rainfall time series for a desired period (e.g., June, early June, July, seasonal etc.) by combining the grid point rainfall over the region. The computed rainfall is correlated with the large-scale climate variables from preceding months and seasons using the NOAA/CDC website (http://www.cdc.noaa.gov/). Regions with high correlation are identified from the correlation maps and indices were created from the corresponding climate variables, which form potential predictor set. The large-scale climate variables included sea level pressure (SLP), sea surface temperature (SST), air temperature at surface level, zonal winds at 500 mb and outgoing long-wave radiation (OLR). In addition predictors based on a rich history of Indian monsoon forecasting efforts (e.g., K Krishna Kumar et al., 1995) were also used.

As a demonstration we considered seasonal rainfall over Gujarat and the All Indian seasonal rainfall. The suite of predictors identified using the correlation analysis described above are listed in the appendix.

Forecast Model – Generalized Linear Model (GLM)

A Generalized Linear Model framework (McCullagh and Nelder 1989) was chosen over a regular linear model for two key reasons – 1) The GLM framework allows the predictors and the predictands to be continuous or discrete or binomial. This allows for the same method to be used for predicting different response variables without sacrificing robustness, 2) The GLM framework has a stepwise procedure based on an Akaikie Information Criteria (AIC) to identify the best subset of predictors. This can easily be implemented in R with built-in functions.

Results – Regional Rainfall Forecast

Data for the 1951–1997 period (first 47 values) is used to fit the GLM. In that, the stepwise procedure is used to identify the best subset of predictors. Thus obtained "best model" is used to predict the 1998-2007 period one year at a time – i.e., data until 1997 is used to predict 1998, data until 1998 is used to predict 1999 and so on. The "year-at-a-time" method was chosen as it allows for a much more realistic forecasting. A sampling of the forecast results are presented below.

First bi-week of June is an important time for crop growth as it is the planting stage, wherein if there are not sufficient wet days and rains, the yield suffers. The forecast of number of wet days (called flood) averaged over the entire country, issued on June 1, is shown in Figure 10. It can be seen that the forecasts are quite good.

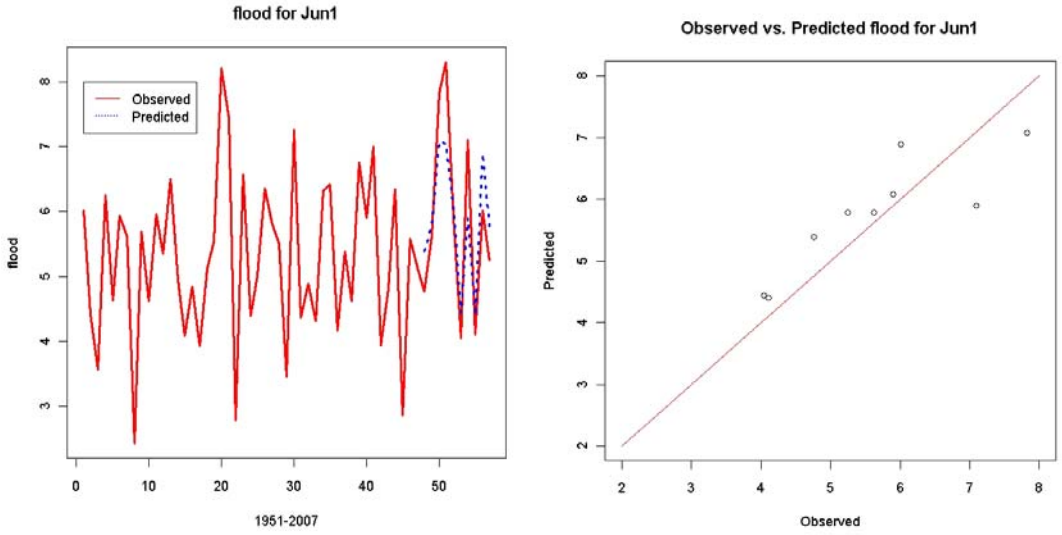

(a) (b)

Fig. 10*: (a) Shows the observed number of flood (wet days shown in red) in the first bi-week of June averaged over all India and the forecast values are shown in blue for the 1998-2007 period (b) shows us the 1:1 relationship between observed and predicted values during 1998-2007.*

* descriptive statistics are R^2 = 0.622, RMSE = 1.02 day
* forecasts for other periods can be found at
http://civil.colorado.edu/~verdina/Predictor%20Plots/

Forecasts of all India seasonal (June-Sept.) total rainfall issued on June 1 are shown in Figure 11. The forecast during the recent period 1998-2007 is quite skillful – especially because the GLM model is able to capture the recent droughts of 2002 and 2004 very well. It can also be useful to know the total seasonal rainfall.

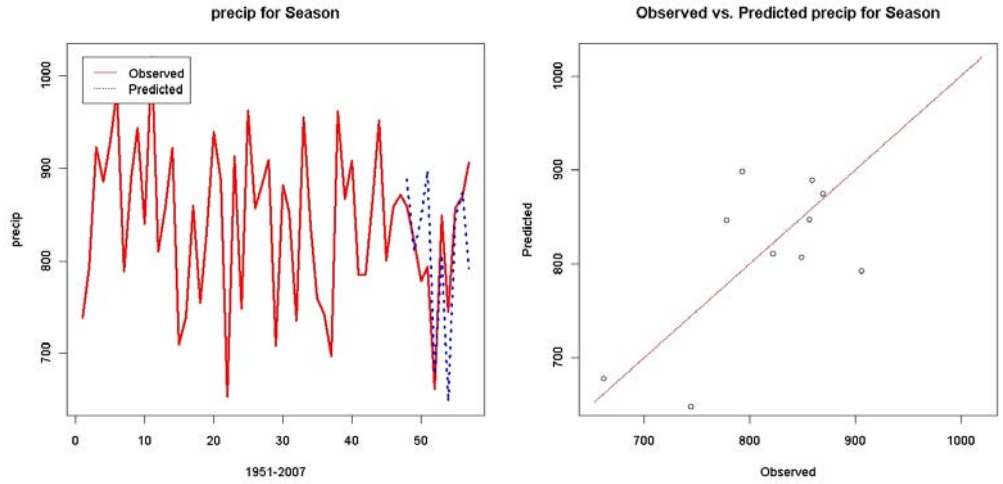

(a) (b)

Fig 11*: Same as Figure 10, but for all India seasonal total rainfall.*

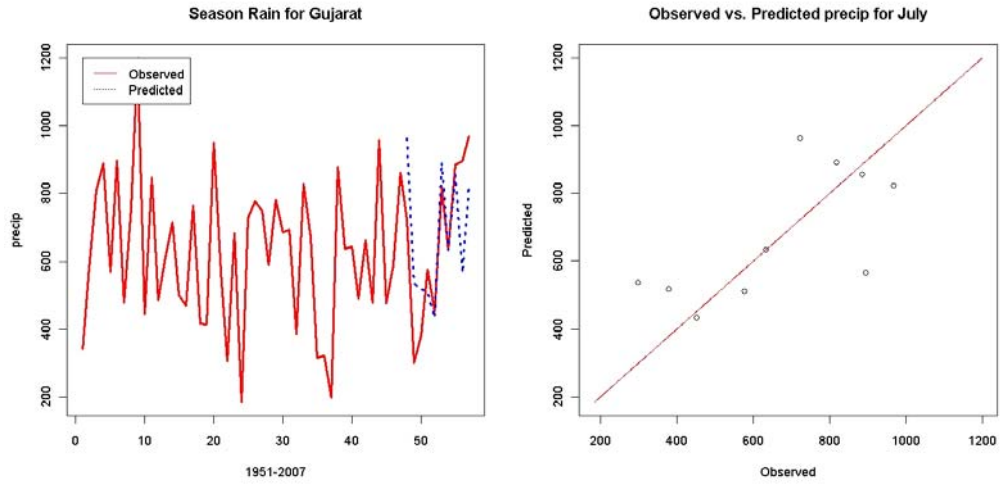

Figure 12*. Same as figure 10 but for July rainfall over Gujarat.*

We also generated forecasts for the July total rainfall over Gujarat region (an important peanut growing region). Here too, the skill in the forecast over the validation period is quite impressive, except in 2006, when the predicted and observed values diverged significantly.

Forecast for the 2009 monsoon season

We applied our forecasting model and generated a forecast of the 2009 June-Sept. all India monsoon rainfall. Interestingly, our model predicts a severe monsoon rainfall deficit (mean forecast of about 650 mm much below the average rainfall of 850 mm).

Unfortunately, the season thus far, seems to be following this forecast and large parts of the country have been declared as drought-affected – this is likely to have significant impact on the crop yield, water resources and also on commodity prices in the coming year.

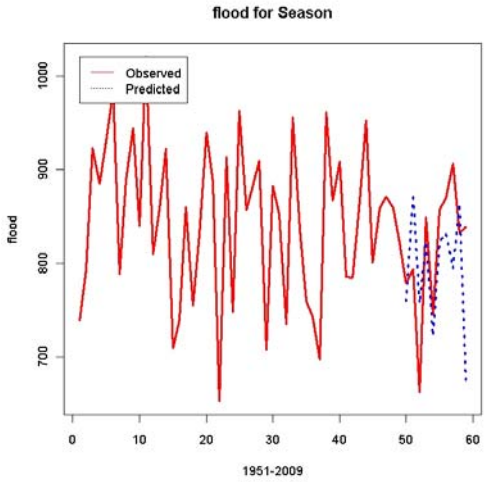

Figure 13. *Same as Figure 10(a), but until 2009.*

Insights into Below Normal Rainfall epochs

The practical value of weekly-monthly rainfall prediction for sub-divisions of India is self-evident. Indeed, some would argue that such information has precedence over information about the 120 day total monsoon rainfall averaged over all of India. Yet, it is with more than a scientific curiosity that our project with USAID has also begun delving into this latter issue, especially to learn whether the secular decline in overall monsoon rainfall that has occurred during the last three decades is transitory, or is perhaps a harbinger of human-induced climate change.

Of particular importance is ensuring that natural variability of all India monsoon rains, when occurring, is not misunderstood to indicate that climate change is either not happening or is happening more intensely than the true human influence. This part of our research is therefore seeking to obtain insights into why the Indian monsoon is in a below normal state for the past three decades. We have examined the role of global sea surface temperature trends in particular being motivated by two considerations: one that Indian monsoon rains are sensitive to the state of global SSTs, and the second that the global oceans are warming as a response to human-induced emissions of GHGs.

Figure 14 shows the year to year variability of all Indian summer monsoon rainfall over the period of 1871–2007, and secular changes are seen from the smoothed green curve which reveals a below normal rainfall epoch since the 1970s. With the present 2009 monsoon season likely to be one of the driest years in recent times, this below normal epoch will continue. This is of great concern to policy makers and planners as it raises the question whether drier conditions will be the "norm" in a warmer world.

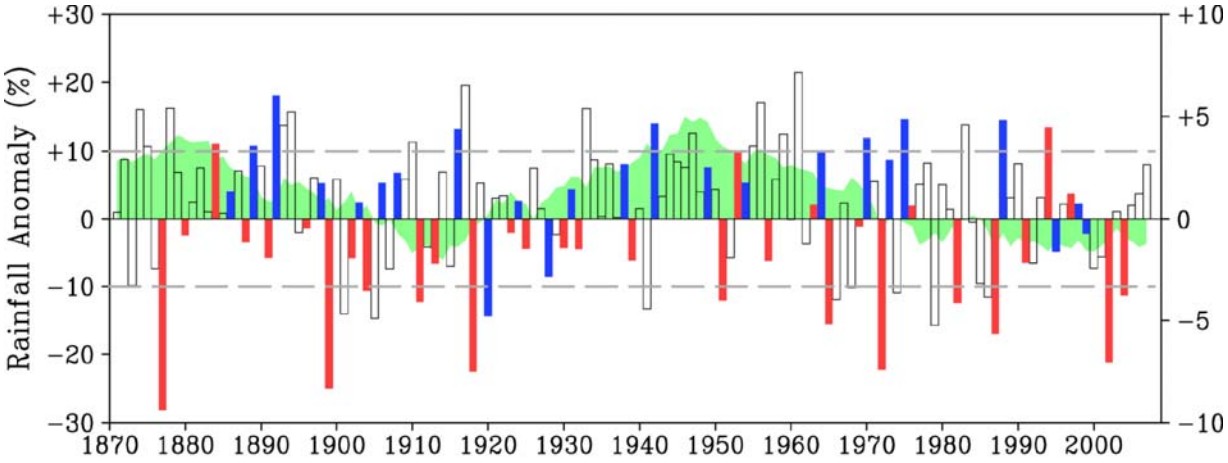

Figure 14. *All-India Summer (JJAS) Monsoon rainfall anomalies (percent of 1961-1990 mean) during 1871-2007. The 31 year sliding mean of the anomalies is shown in green shaded curve. The red/blue bars indicate El Nino/La Nina years, respectively.*

The observed trends of the oceanic surface temperatures during 1977-2006 show a general warming over much of the globe (Figure 15). Conspicuous has been an absence of warming along the equatorial Pacific from the dateline to South America and an expanse of the east Pacific between 30°N and 30°S, somewhat reminiscent of the La Niña condition. By contrast, coupled models simulate a relatively uniform pattern of SST warming using observed and projected greenhouse gas (GHG) concentrations and other forcings (IPCC, 2007). Based on the well known monsoon-ENSO teleconnections (Kumar et al., 1999 and references therein) La Nina tends to favor good monsoon rains – but this has not been the case during recent decades, and the question we explore is whether other aspects of regional SST change (perhaps attributable to human-induced causes) have been important.

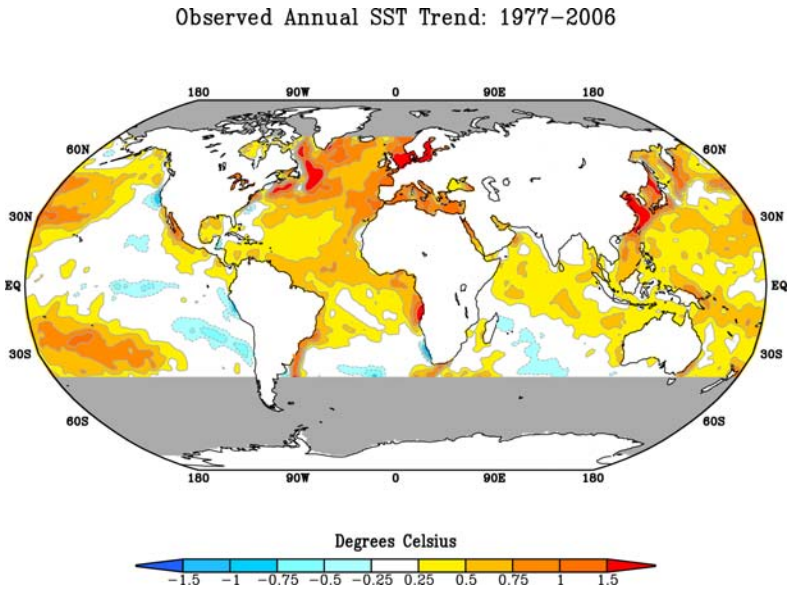

***Figure 15**. Annual SST trend for the period of 1977-2006.*

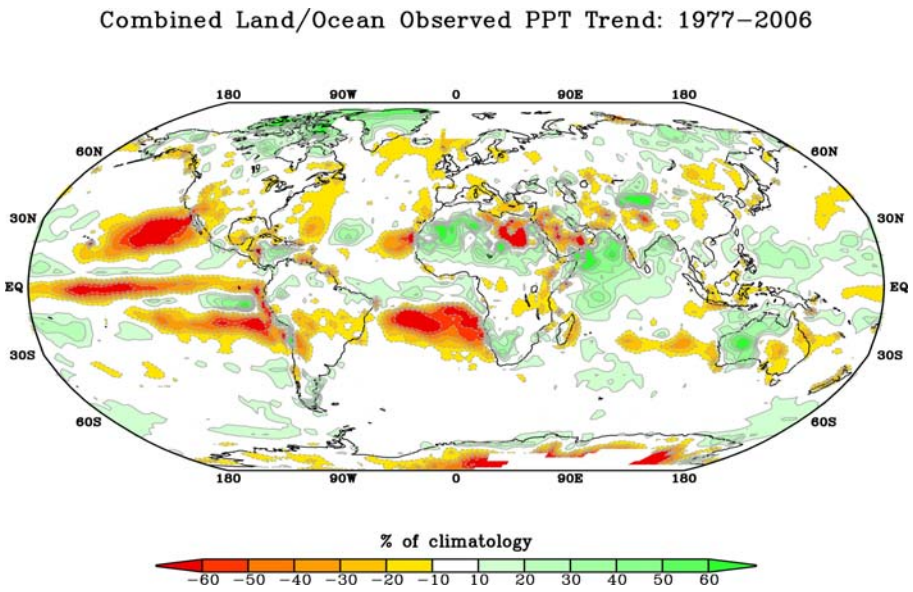

***Figure 16**. Same as Figure 15 but for the precipitation over land and ocean. The climatology is based on 1979-2006 period.*

Precipitation trends over land and ocean during the same period (Figure 16) show the diminished rainfall over India, as well as other areas including the Southwestern U.S. and the Southeast Australia. We note that this period of declining Indian rainfall has occurred together with a recovery in rains over the Sahel.

To understand the lower rainfall epoch over India we used three atmospheric general circulation models (AGCMs : CCM3, NCEP-GFS and GFDL) and forced them with the observed SST trend pattern as shown in Figure 15. The three model average precipitation response to this forcing (Figure 17) shows a pattern that is similar to the observed trend pattern seen above.

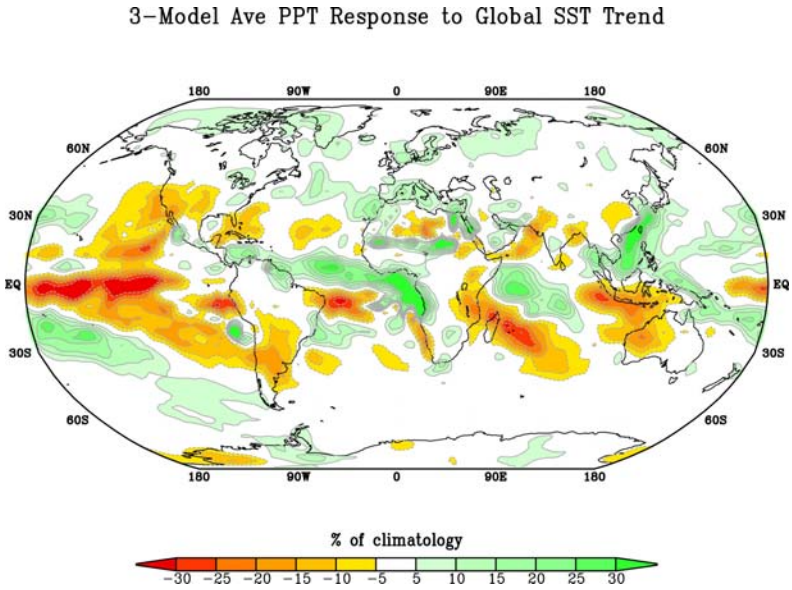

Figure 17*. Same as Figure 16, but from three model average response to global SST forcing.*

This indicates that the global precipitation pattern during the recent three decades and the decreasing Indian monsoon rainfall in particular are at least qualitatively consistent with an influence being exerted by global SST patterns during this period. The question is, which SST patterns are important?

To further understand the sensitivity identified in Fig. 17, we performed additional simulations to assess the role of two particular aspects of tropical SST change: one is the warming trend of the Indo-west Pacific Ocean, and the other is the warming of the tropical Atlantic. Other research has indicated that each of these regional warmings are likely the result of the ocean's response to GHG forcing.

In the first set of experiments the AGCMs were forced by the SST pattern in the tropical western Pacific and Indian ocean regions only (we call it the "warm pool" region) while maintaining climatological SSTs elsewhere. The three model average precipitation response from this experiment (Figure 18) seems to fairly well capture the drying pattern over India. The suggestion from these runs is that the semiarid regions of India in the north may be experiencing a secular decline in rainfall attributable to a warming of SSTs in the oceans in immediate proximity to India.

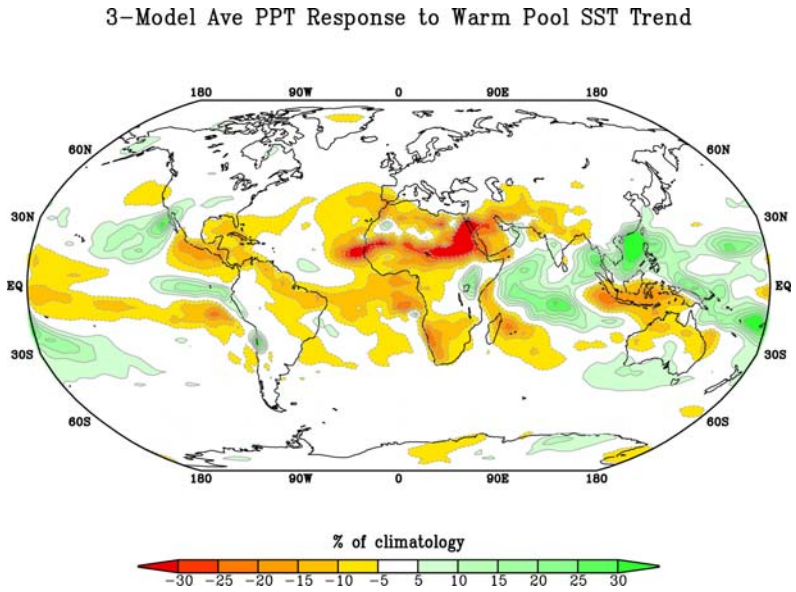

Figure 18. *Same as Figure 17 but from warm pool SST forcing.*

In the second set of experiments the AGCMs were forced by the SST pattern in the tropical Atlantic Ocean region only while maintaining climatological SSTs elsewhere. The three model average precipitation response from this experiment (Figure 19) shows a pattern that dries the humid south portions of the subcontinent, and much of the adjacent seas. This pattern is in most ways opposite from the observed trend over the India region and adjacent seas, but the results are nonetheless very interesting for illustrating that the far-a-field Atlantic Ocean can materially excite the Indian monsoon. The fact that this signal fails to match the observed pattern of change need not diminish its significance, and may indicate that other factors (perhaps the warm pool effect, or cool Pacific SSTs) have counterbalanced this Atlantic influence.

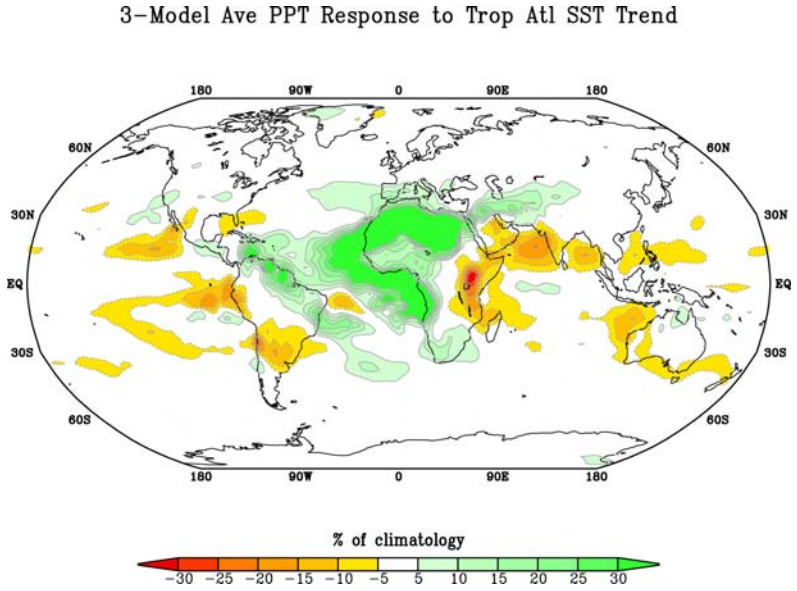

Figure 19. *Same as Figure 18, but from tropical Atlantic SST forcing.*

To highlight the rainfall over the land portion of India only, we computed the model precipitation at all the land points over the Indian subcontinent and created a Probability Density Function (PDF) based on the numerous individual simulations (~100) conducted for all the three SST forcings (Fig 20). As seen before, the observed precipitation trend pattern (Figure 16) is well reproduced by our experiments using global SST forcing (Figure 17). It is therefore not surprising that the observed decline of about -5 percent during 1977-2006 is consistent with the shift in probability to dry conditions due to the trend in global SSTs as shown by the black curve in Fig. 20. Interestingly, the PDFs for the Atlantic trend forced experiments (red curve) largely reproduce the results based on global SSTs, suggesting that the all-India drying may be especially linked with Atlantic ocean warming.

We have yet to reconcile this result with the fact that *the spatial pattern* of rainfall responses to Atlantic warming do not match the observed trend pattern. It is also apparent that the observed drying could be argued to be consistent with the statistical distribution of rainfall anomalies occurring in response to the warm pool warming (green curve) as readily as with the Atlantic Ocean warming. What is important to take away from these analyses is that there is a wide range of outcomes for the Indian monsoon for identical forcing, implying that there may exist only a modest predictable signal of change due to forcing. We note, for instance, that the 1977-2006 Indian monsoon rainfall trend due to GHG forcing, which we have calculated from the IPCC Fourth Assessment models (CMIP), shows virtually no response (blue tick in Fig. 20). To be sure, we suspect that some of the spread of the PDFs stems from a co-mingling of different models, each of which has its own unique sensitivity. The observed system may therefore be more constrained by SST changes than implied by the preliminary analysis we have done for this project.

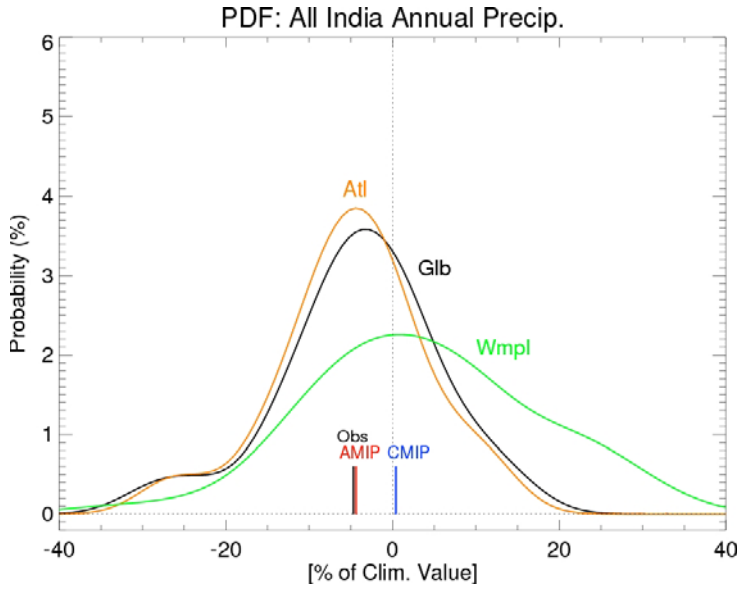

Figure 20*. PDF of all Indian annual precipitation (only the land points) from the model ensembles for the three different SST forcing. ATL (Atlantic), GLB (Global) and Wmpl (Warm Pool).*

Summary and Conclusions

Analyses of subnational, within-season variations in Indian monsoon rainfall were performed, with a number of significant results.

Diagnostic Analyses

Using a recently released daily, gridded national rainfall data set at 0.5 degree resolution (about 50 km) for the period 1951-2007, the following significant rainfall events and characteristics were investigated and mapped (along with several others):

- Wet spell probability in July, a key period of crop maturation
- Biweekly probability of transition from wet to dry, and dry to wet spells
- Seven day annual maximum rainfall, an important seasonal event for soil moisture replenishment, was mapped and inter-annual trends computed
- Crop specific rainfall deficits, and trends in the same
- Seasonal cumulative rainfall, and trends in timing

These analyses revealed the following:

- A general drying trend during the monsoon months (July, August in particular), vital for crop maturity, over much of the Indian subcontinent.
- Increased rainfall during pre-monsoon months (April, May and also in June). But the pre-monsoon increase does not compensate for the monsoon rainfall decrease. Pre-monsoon increase in land surface vegetation primarily due to irrigation (Lee et al., 2008) is strongly hypothesized as a reason for this phenomenon. This needs to be explored further as there seems to be a potential for unintended consequences of developmental policies.
- The extreme rainfalls also show a significant decrease over the country. The occurrence of extreme events are important for sub-surface water replenishment and also for filling up of surface reservoirs, that is crucial for water resources and agriculture.
- Significant rainfall deficit with respect to rice is seen in the peninsular region and also over Northern and Northwestern parts of the country. These also show significant increasing trends. Much less deficit is seen over Northeastern parts of the country and also in the eastern Gangetic plains. This information can be of immense use in devising sustainable cropping policies.
- Transition probabilities during the June and July show a strong association with ENSO. These can be used in generating weather sequences that could be coupled with crop models to provide yield forecast and consequently, help devising seasonal mitigation strategies.

Risk Prediction

For agriculturally significant sub-national areas and within season periods (e.g., planting during the first bi-week of June), statistical analyses were performed to develop predictive models using global climate system variables (like SST, OLR, SLP) as predictors. Our analysis indicates the following:

- The use of GLM-based approach for monsoon rainfall forecasting is proving to be an attractive alternative to the existing statistical models. The GLM approach has the versatility to produce forecasts of discrete variables (such as wet days, dry days, etc.) and also continuous variables (such as weekly, monthly, seasonal

precipitation).This framework can also be used to produce forecasts of extreme events (Katz et al., 2002).

- We found the GLM models to be quite skilful in our application to the rainfall forecast of first bi-week of June, seasonal rainfall for Gujarat, all-India seasonal total rainfall and number of wet days over India in the first bi-week of June. We also applied this to generate a forecast for the June-Sept. 2009 monsoon, and a severe deficit was forecasted. This unfortunately is turning out to be the reality this year.

Investigation of Secular Trends

Variability of the all Indian monsoon was investigated over the period 1871-2001 for century scale (secular) trends. Below normal rainfall has been the norm since 1970. This same period saw significant warming of the oceans due to GHGs. As the Indian monsoon is well known to be sensitive to the state of global SSTs, a series of experiments using atmospheric global circulation models was conducted. Warming trends in both the Indo-West Pacific Ocean warm pool and the tropical Atlantic have explanatory potential. Our idealized modeling experiments suggest the following

- The global SST trends, especially of the tropical oceans, seem to be a significant modulator of monsoon rainfall at multi-decadal time scales. The warming of the tropical oceans seems to be producing a below normal monsoon epoch.
- This is somewhat counter intuitive to the notion that warmer oceans provide more moisture in the atmosphere and consequently, more rainfall. We find that the "relative" strength of warming and the gradients in the SSTs are extremely important for steering the moisture to the land regions. This was seen in the IPCC model SST trends which exhibit a uniform warming of the tropical oceans during the recent observational period and the atmospheric models respond by enhanced rainfall over the Indian subcontinent.
- The warming in tropical Atlantic and tropical Indian Ocean (including Western Pacific) seem to be strong "push buttons" for producing drier epochs over India.
- Thus, the simulated future state of the Indian monsoon will depend largely on the models' ability to capture realistic tropical ocean SST variations.

References

Apipattanavis, S, G. Podesta, B. Rajagopalan and R. Katz, A semiparametric multivariate and multisite weather generator, *Water Resources Research,* 43(W03432), 2007

Apipattanavis, S., 2008. 2008. Stochastic Nonparametric methods for multi-site weather generation and flood frequency estimation: applications to construction delay, hydrology and agricultural modeling, PhD dissertation, University of Colorado, Boulder, CO, 2008.

IPCC (2007), *Climate Change 2007 - The Physical Science Basis* Contribution of Working Group I to the Fourth Assessment Report of the IPCC (ISBN 978 0521 88009-1
Hardback; 978 0521 70596-7 Paperback)

Katz, R. W., M. B. Parlange, and P. Naveau (2002), Statistics of extremes in hydrology, *Adv. Water Resour.*, *25*, 1287-1304.

Kumar KK, Soman MK, Rupa Kumar K, (1995) Seasonal forecasting of Indian summer monsoon rainfall. *Weather* 50:449-467.

Lee, E., T. Chase, and B. Rajagopalan, R. G. Barry, T. W. Biggs and P. J. Lawrence, Effects of irrigationi and vegetation activity on early Indian summer monsoon variability, *International Journal of Climatology*, doi: 10.1002/joc.1721, 2008.

Mccullagh, P., and J. A.Nelder, (1989). *Generalized Linear Models*. London; New York: Chapman and Hall.

Podesta, G., et al (2009), Decadal climate variability in the Argentine Pampas: regional impacts of plausible climate scenarios on agricultural systems, (in press), *Climate Research.*

Rajeevan, M., J. Bhate, J. D. Kale, B. Lal, Current Science, 91, 296 (2006).
Wiks, D., Statistical methods in the atmospheric sciences (2006), *Academic Press,*

Appendix

R-Codes

All the R-codes developed as part of the study to perform Tasks A and B are listed and described below. The codes are fairly straightforward and can be easily followed and replicated with the comments inside the codes. They can all be found at http://civil.colorado.edu/~verdina/R%20Codes/

binary_droughtDEUX.txt	transform daily rainfall into binary (1 = dry)
binary_dryspell.r	initialize matrix for length of wetspell by station
binary_wetspellCOUNT.txt	compute number of wet events
binary_wetspellDEUX.r	transform daily rainfall into binary (1 = wet)
deficit.r	compute/plot crop rain deficit
drywetdays_byregion.r	compute wet and dry day count by region
extreme.r	compute/plot extreme rainfall events
extremecount.r	compute number of extreme events
gujpred.r	predict total Gujarat seasonal rainfall
julian.txt	compute/plot user-specified Julian day
junejulyrain.r	compute total rainfall for Jun/Jul
lengthdryspells.r	compute length of dry spells by region
lengthwetspells.r	compute length of wet spells by region
loadgujarat.r	load predictors for Gujarat rain prediction
may_to_sep_totals.r	cumulative monthly rainfall totals
plotriskmapsallvsENSO.txt	user-specified risk map output
pred.r	predict all-India total Jun/Jul rainfall
predictors.r	narrow down potential predictors for 'pred.r'
prob2.txt	compute probability dist. for wetspell all years
prob2ENSO.txt	compute probability dist. for wetspell ENSO years
seasonpred.r	predict all-India total seasonal rainfall
sevendaymax.r	compute/plot
tessst.r	computes wetspells by region for specified month
transitions.txt	compute/plot prob. dist. of changing weather (wet-dry)
transitions22.txt	same as transitions.txt with ENSO year option
wet_plots.r	compute/plot avg wet days by month
wetspellprob.r	compute/plot wetspell probability dist.
yeartotals.txt	compute total yearly rainfall by station

Gujarat Rainfall Predictors List

dectemp - 500 hpa temperature lat -5.0 to 5.0 lon 10.0 to 15.0 season 29 PDEC

djfgpm1 - 850 hpa height(gpm) lat -32.5 to -27.5 lon 122.5 to 132.5 season 15 DJF

djfgpm2 - 700 hpa height(gpm) lat -35.0 to -30.0 lon 120.0 to 125.0 season 15 DJF

djfgpm3 - 1000 hpa height(gpm) lat -35.0 to -30.0 lon 130.0 to 135.0 season 15 DJF

djfpres - msl pressure lat -35.0 to -25.0 lon 125.0 to 140.0 season 15 DJF

djftemp - 500 hpa temperature lat -5.0 to 5.0 lon 5.0 to 15.0 season 15 DJF

djfzon1 - 1000 hpa zonal wind lat 20.0 to 25.0 lon 60.0 to 70.0 season 15 DJF

djfzon2 - 850 hpa zonal wind lat -15.0 to -10.0 lon 105.0 to 120.0 season 15 DJF

djfzon3 - 700 hpa zonal wind lat -10.0 to -5.0 lon 105.0 to 110.0 season 15 DJF

febtemp - 200 hpa temperature lat 0.0 to 5.0 lon 130.0 to 140.0 season 2 FEB

febzon1 - 1000 hpa zonal wind lat 20.0 to 25.0 lon 62.5 to 70.0 season 2 FEB

febzon2 - 1000 hpa zonal wind lat -15.0 to -10.0 lon 110.0 to 115.0 season 2 FEB

febzon3 - 850 hpa zonal wind lat -12.5 to -7.5 lon 105.0 to 115.0 season 2 FEB

febzon4 - 850 hpa zonal wind lat 2.5 to 7.5 lon 132.5 to 142.5 season 2 FEB

febzon5 - 700 hpa zonal wind lat -2.5 to 5.0 lon 105.0 to 115.0 season 2 FEB

febzon6 - 500 hpa zonal wind lat -2.5 to 2.5 lon 85.0 to 90.0 season 2 FEB

febzon7 - 500 hpa zonal wind lat -2.5 to 2.5 lon 105.0 to 110.0 season 2 FEB

febzon8 - 500 hpa zonal wind lat 57.5 to 62.5 lon 45.0 to 50.0 season 2 FEB

jangpm1 - 850 hpa height(gpm) lat -32.5 to -27.5 lon 115.0 to 125.0 season 1 JAN

jangpm2 - 700 hpa height(gpm) lat -30.0 to -25.0 lon 115.0 to 125.0 season 1 JAN

janmerw - 1000 hpa meridionl wind lat -2.5 to 2.5 lon 145.0 to 150.0 season 1 JAN

janpres - msl pressure lat -35.0 to -30.0 lon 115.0 to 125.0 season 1 JAN

jantemp1 - 500 hpa temperature lat -2.5 to 5.0 lon 37.5 to 42.5 season 1 JAN

jantemp2 - 500 hpa temperature lat -5.0 to 5.0 lon 10.0 to 15.0 season 1 JAN

jantemp3 - 200 hpa temperature lat -20.0 to -10.0 lon 160.0 to 170.0 season 1 JAN

Season Rainfall Predictor List

jun200h - 200hPa height lat 30-40N, lon 70-80E, P-Jun x-grids 29.- 33. ygrids 49.- 53. season 23
jun200h2 - 200hPa height lat 32.5-37.5N, lon 70-80E, P-Jun x-grids 29.- 33. ygrids 50.- 52. season 23
jun200m - 200hPa merid wind lat 20-30n, 85-90E, P-Jun x-grids 35.- 37. ygrids 45.- 49. season 23
jun200z - 200hPa zonal wind lat 42.5-47.5N, lon 70-80E, P-Junx-grids 29.- 33. ygrids 54.- 56. season 23
jun500m - 500hPa merid wind lat 15-20N, lon 235-240E, P-Jun x-grids 95.- 97. ygrids 43.- 45. season 23
juntemp - 700hPa temp lat 20-25N, lon 245-250E, P-Jun x-grids 99.-101. ygrids 45.- 47. season 23
juntemp2 - 500hPa temp lat 10S-5S, lon 260-275E, P-Jun x-grids105.-111. ygrids 33.- 35. season 23
mam200h - 200hPa height lat 25S-20S, lon 40-50E, MAM x-grids 17.- 21. ygrids 27.- 29. season 16
mam200z - 200hPa zonal wind lat 15S-5S, lon 30-40E, MAM x-grids 13.- 17. ygrids 31.- 35. season 16
mam500z - 500hPa zonal wind 0-10N, 255-265E, MAM x-grids103.-107. ygrids 37.- 41. season 16
mam700h - 700hPaheight lat 22.5-27.5N, lon 197.5-202.5E,MAM x-grids 80.- 82. ygrids 46.- 48. season 16
mampres - 60msl-pres Lat 7.5N-20N lon 75E - 80E MAM x-grids 31.- 33. ygrids 40.- 45. season 16
mampres2 - 60msl-pres Lat 15-25N, lon 195 to 205E MAM x-grids 79.- 83. ygrids 43.- 47. season 16
mamtemp - 200hPa temp lat 17.5-22.5N, lon 90-100E, MAM x-grids 37.- 41. ygrids 44.- 46. season 16
mamdjf200m - 200hPa merid wind Lat 15S-5S, lon 140-150E, MAM-DJF x-grids 57.- 61. ygrids 31.- 35. season 17
mamdjf700h - 700hPa height lat 25S-20S, lon 105-110E, MAM-DJF x-grids 43.- 45. ygrids 27.- 29. season 17
mamdjfpres - 60msl-pres lat 20S to 10S, lon 130E- 150E MAM-DJF x-grids 53- 61 ygrids 29- 33 season 17
mamdjfpres2 - 60msl-pres lat 17.5S - 12.5S lon 140E-150E MAM-DJF x-grids 57- 61 ygrids 30- 32 season 17
mamdjftemp - 1000hPa temp 0-10N, 200-210E, MAM-DJF x-grids 81- 85 ygrids 37- 41 season 17
mar700m - 700hPa merid wind lat 17.5-25N, lon 310-315E, Mar x-grids125-127 ygrids 44- 47 season 3
martemp - 500hPa temp lat 25S-20S, lon 70-80E, Marx-grids 29- 33 ygrids 27- 29 season 3
may200z - 200hPa zonal wind lat 60-70N, lon 90-100E, P-May x-grids 37- 41 ygrids 61- 65 season 22

may200z2 - 200hPa zonal wind lat 0-10N, lon 220-230E, P-May x-grids 89- 93 ygrids 37- 41 season 22
may500z - 500hPa zonal wind lat 5-10N, lon 255-265E, May x-grids103.-107. ygrids 39.- 41. season 5
may850z - 850hPa zonal wind lat 5-10N, lon 185-200E, May x-grids 75.- 81. ygrids 39.- 41. season 5
maypres - 60msl-pres lat 7.5N to 20N, lon 75E to 80E May x grids 31.- 33. ygrids 40.- 45. season 5
maypres2 - 60msl-pres lat 15 N-25N, lon 195E-205E May x-grids 79.- 83. ygrids 43.- 47. season 5
maytemp - 1000hPa temp lat 25-30N, lon 75-80E May x-grids 31.- 33. ygrids 47.- 49. season 5
maytemp2 - 700hPa temp 2.5-7.5N, lon 55-60E, May x-grids 23.- 25. ygrids 38.- 40. season 5
maytemp3 - 700 hPa temp lat 12.5-17.5N, 72.5-77.5E May x-grids 30.- 32. ygrids 42.- 44. season 5
maytemp4 - 200 hPa temp lat 15-25N, lon 90-95E May x-grids 37.- 39. ygrids 43.- 47. season 5